Radio-frequency susceptibility apparatus for measuring small superconducting samples

B. J. Dalrymple and D. E. Prober

Becton Center, Section of Applied Physics, P. O. Box 2157, Yale University, New Haven, Connecticut 06520

(Received 19 September 1979; accepted for publication 20 February 1984)

A radio-frequency magnetic susceptibility apparatus is described, which is capable of measuring the superconducting transition temperature of individual samples with volumes as small as 2×10^{-8} cm^3 (mass $\simeq 0.1$ μg) with a signal-to-noise ratio of 20. The system uses phase-sensitive detection and operates between 1 and 10 MHz. Measurements in large dc magnetic fields ~ 150 kG are also possible. Detailed information concerning construction and operation is provided.

PACS numbers: 74.30.Ci, 74.10. + v, 07.55. + x

INTRODUCTION

In the synthesis and characterization of new superconducting materials, it is often desirable to measure the transition temperature and critical magnetic field properties of small single-crystal samples. Indeed, for many newly synthesized compounds, only very small crystals may be available, or such smaller crystals may be more perfect than larger samples. Measurements on such very small crystals require a method of detecting the superconducting phase boundary, which has excellent resolution and operates over a wide range of fields and temperatures.

This paper reports the development of a very sensitive ac magnetic susceptibility apparatus. The technique involves placing the sample in a coil which is part of a parallel LC circuit and measuring the shift in the resonant frequency to detect changes in the sample susceptibility. This apparatus is sensitive enough to measure the superconducting transition of a 130-ng sample with a signal-to-noise ratio of 20. The cryogenic apparatus is of simple construction. Operation is simple and reliable. The cryogenic probe is small enough to fit into a liquid–helium storage Dewar, facilitating rapid and economical determination of zero-field transition temperatures (for $T_c > 4.2$ K). In addition, the system is compatible with operation in dc magnetic fields of at least 150 kG.

This paper is organized as follows. In Sec. I we discuss the various techniques for measuring the superconducting transition. The basic principles of the technique we have developed are presented in Sec. II. We then discuss in Sec. III the electronic circuitry, the cryostat, and other experimental details. The performance of the system is examined in Sec. IV. While the principles of our technique are relatively straightforward, we give a detailed description of the cryogenic apparatus and electronic circuitry, since these details are important for obtaining optimum performance.

I. METHODS FOR DETERMINING SUPERCONDUCTING TRANSITIONS

The three techniques which have been most widely used to detect the superconducting-to-normal phase transition are measurements of the resistivity, the heat capacity, and the magnetic susceptibility (or magnetization). Resistivity measurements are often the easiest to make. However, resistivity measurements are the least reliable, as a single superconducting path in an otherwise nonsuperconducting sample can give the appearance of bulk superconductivity. For very small samples, connection of the electrical leads is an additional problem.

Heat-capacity measurements are, in principle, the most reliable method for determining the transition temperature, as they are true bulk measurements. However, heat-capacity measurements on very small samples require complicated calorimeters and cryostats.[1,2] Small-sample heat-capacity measurement techniques have recently been reviewed by Stewart.[3] The calorimeters developed to date have optimum sensitivity only for thin-film samples deposited directly onto the calorimeter, because the internal thermal relaxation times are short and good thermal contact to the calorimeter is assured. For thin-film samples deposited on the calorimeter, the smallest sample for which the superconducting transition can be measured[3] is ~ 10 μg. For single-crystal samples attached to the calorimeter, such sensitivity is not easily achieved, due to the addenda heat capacity (of the thermal bonding agent) and related thermal boundary resistance(s). In addition, operation of any such calorimeter in large magnetic fields can be difficult, due to the effect of the magnetic field on thermal and electrical conductances.[3] Thus, heat-capacity measurements are currently not suitable for detecting the superconducing transition, in a magnetic field, of small single crystals of mass < 1 μg.

Measurements of the magnetic susceptibility detect the diamagnetism of the superconducting state. Ideal type-I superconductors are fully diamagnetic for applied fields less than the critical field $H_c(T)$.[4] (Here we ignore demagnetizing effects and also field penetration into the sample a distance equal to the magnetic field penetration depth λ, typically of order 0.1 μm.) Ideal type II superconductors show full diamagnetism only below the lower critical field $H_{c1}(T)$. For fields between $H_{c1}(T)$ and the upper critical field $H_{c2}(T)$, the magnitude of the dc magnetization decreases uniformly to the normal-state value. In order to detemine $H_{c2}(T)$ from this magnetization curve, one must detect the change in slope of the magnetization curve at $H_{c2}(T)$. This change in slope is small for both ideal and real high-κ type-II superconductors (κ is the Ginzburg–Landau parameter[4]).

It is fortunate that many real type-II superconductors remain at least partially diamagnetic to low-amplitude, low-

 0034-6748/84/060958-06$01.30 © 1984 American Institute of Physics

frequency ac magnetic fields in the mixed state $[H_{c1}(T) < H < H_{c2}(T)]$, and display a single, sharp transition in the ac susceptibility at the upper critical field $H_{c2}(T)$[5] [or if surface superconductivity is important, at $H_{c3}(T)$]. The partial diamagnetism seen up to H_{c2} (or H_{c3}) can be caused by an intrinsic surface barrier to flux entry[6] and/or by flux pinning. The sharp transition in the ac susceptibility data can be used to measure $H_{c2}(T)$, once it is established (e.g., by heat-capacity measurements) that the feature in the ac susceptibility data indeed corresponds to $H_{c2}(T)$. This correspondence is easily demonstrated for the layered transition-metal dichalcogenide samples which we have studied,[7] where heat-capacity measurements have been made[8] on substantially larger ($>$ 1 mg) crystals of the same compounds as we have studied.

A potential problem for ac susceptibility measurements concerns sample inhomogeneities. If the sample contains randomly distributed T_c values, a smeared out transition will be observed. It is possible that the sample's interior inhomogeneities can be completely masked by a uniform surface layer with a higher T_c. This is not a problem for the single-crystal samples we have studied. In any case, ac susceptibility measurements are, in general, less likely to be in error due to inhomogeneities than are resistivity measurements, since ac susceptibility measurements require a complete superconducting loop to produce shielding rather than just a single superconducting path.

Several techniques have been developed for measuring the ac susceptibility of small samples, but all techniques, including the one reported here, must deal with the difficulty of coupling to the small sample volume. Techniques developed previously include direct measurements of the self- or mutual inductance of a pickup coil enclosing the sample[9] and measurement of the resonant frequency of low-frequency resonant circuits[10] or of radio-frequency tunnel diode oscillators.[11] Nonresonant measurements of inductance are, in general, less sensitive than resonant techniques by approximately a factor of Q (the resonant-circuit quality factor), if the same ac field amplitude is used. Use of a cooled resonant transformer to increase the signal amplitude is possible,[9(a)] but is generally incompatible with operation in large dc fields.

Resonant circuits can use small inductances to couple efficiently to the sample. However, for low resonant frequencies (less than $\sim$ 100 kHz), the cable resistance severely limits the circuit Q when a room-temperature capacitor is used. Use of a room-temperature capacitor may be necessary due to the large electrical (and physical) size of the required capacitance. For high resonant frequencies (greater than $\sim$ 1 MHz), a tunnel diode oscillator can achieve excellent resolution and stability in determining the LC self-resonant frequency.[12] However, this is not a simple technique for use at low ac field levels and with small inductances, due to the relatively small impedance at resonace, given by $Z_{LC} = Q\omega_r L$. In addition, the magnetoresistance of the inductor coil leads to the requirement of different diode biasing and/or loading at different magnetic field values (to obtain oscillation). This is also true of other marginal oscillators. We conclude that while ac susceptibility measurements can offer excellent sensitivity, none of these other ac susceptibility methods appear to be promising for the application we have addressed—measuring the ac susceptibility transitions of very small samples in small and also in large dc magnetic fields. The ac susceptibility technique we have developed does provide this capability.

II. DETECTION TECHNIQUE

This section describes the basic principles of operation of the ac susceptibility apparatus. To determine changes in the sample's ac susceptibility, the sample is placed inside a coil which is part of a high-Q ($Q > 30$) parallel resonant circuit. This circuit is driven by a radio-frequency current source. When the sample is superconducting and the applied dc field is zero, the ac field is fully shielded from the sample's interior. The ac field penetration is limited to the superconducting penetration depth λ, which is approximately 0.1 μm for a typical material. After the sample passes from the superconducting to the normal state, i.e., as the temperature is raised, the ac field penetrates into the sample a much larger distance equal to the normal-state skin depth δ. This distance is material dependent; for our samples it is of the order of 100 μm at 3 MHz. Thus, at the transition there is a change in the effective sample volume from which the ac field is excluded. This alters the coil inductance, and shifts the resonant frequency.

The shift in resonant frequency when the sample goes from the superconducting state to the normal state can easily be calculated. We consider the case where the ac field is fully excluded from the sample below T_c, and fully penetrates the sample above T_c, in order to obtain the simplest estimate of the system's sensitivity. The inductance of the coil can be written as $L = L_0(1 + \eta\chi)$ (mks units), where L_0 is the inductance of the coil when empty, χ is the sample susceptibility, and η is the effective filling factor. For a sample which is completely diamagnetic in the superconducting state $\chi = -1$; for this case η is given approximately by

$$\eta \simeq d_s^3/2V_{\text{coil}}. \tag{1}$$

This result is for a thin platelet of face diameter d_s (see Fig. 2), with the ac field perpendicular to the sample face. The result in Eq. (1) includes the demagnetizing effects for $\chi = -1$. For complete ac field penetration above T_c, $\chi = 0$. Thus, for our simple estimate we obtain $\Delta L = \eta L_0$, with η given by Eq. (1).

For a small sample $\eta \ll 1$, and the superconducting-to-normal transition results in a small shift in resonant frequency Δf_r, given by

$$\frac{\Delta f_r}{f_r} \simeq \frac{-\Delta L}{2L_0} = \frac{-\eta}{2} \simeq \frac{-d_s^3}{4V_{\text{coil}}}. \tag{2}$$

Using typical values of $f_r = 3$ MHz, $d_s = 100$ μm, and $V_{\text{coil}} = 1$ mm^3, we obtain $\Delta f_r = 750$ Hz. This shift is easily measured.

The shift in resonant frequency is measured using a phase-sensitive detection scheme which produces an output voltage proportional to the imaginary, or out-of-phase, component of the LC circuit impedance. We denote this imaginary component as Z_2; the total impedance is given by

$Z_{LC} = Z_1 + jZ_2$. The imaginary component of Z_{LC} is shown in Fig. 1 as a function of the applied frequency f_a. Z_2 is zero at resonance, and varies linearly with frequency near resonance. With the circuit biased at a fixed frequency near resonance $f_a = f_0$, the imaginary part of the impedance and thus the output voltage V_0 will change from point B to point A as the sample goes from the superconducting to the normal state.

The phase-sensitive detector used to measure Z_2 is shown in Fig. 2 in block diagram form; a full circuit diagram is shown below in Fig. 3. Referring to Fig. 2, the resonant circuit is biased with a constant current by the capacitor $C_1 = 1\ pF$, which forms a rf current source with the rf voltage generator, since the impedance of C_1 is much larger than the LC circuit impedance. The rf current $I_1 \simeq j\omega_a C_1 V_g$ is shifted 90° in phase relative to the generator voltage V_g. The voltage appearing across the resonant circuit is given by $V_{LC} = Z_{LC} = I_1 = (-Z_2 + jZ_1)\omega_a C_1 V_g$. This voltage is amplified and fed to the balanced mixer. The local oscillator input of the mixer (L in Fig. 3) is driven by V_g. The mixer output (X in Fig. 3) contains a dc voltage component proportional to any signal present at its input which is in phase with the ac voltage at the local oscillator input port. The mixer output will, therefore, have a dc component proportional to Z_2. (Components at the harmonics of f_a are also present, but these are removed by a low-pass filter.) The change in resonant frequency has thus been turned into a change in dc output voltage.

The slope of the imaginary component of Z_{LC} at resonance can easily be calculated. The change in output voltage along the linear portion of the transfer curve for a given change in resonant frequency can be shown to be

$$\Delta V_0 = -4\pi\beta L_0 Q^2 |I_1| \Delta f_r. \tag{3}$$

Here $|I_1|$ is the magnitude of the rf biasing current and β is the product of the gains of the rf amplifier, the balanced mixer, the low-pass filter, and the dc amplifier. The Q can be determined by measuring the resonant frequency f_r and the frequencies of the positive and negative peaks of the output signal (Fig. 1), with the sample either superconducting or normal. Q is given by f_r divided by the difference of the two peak frequencies.

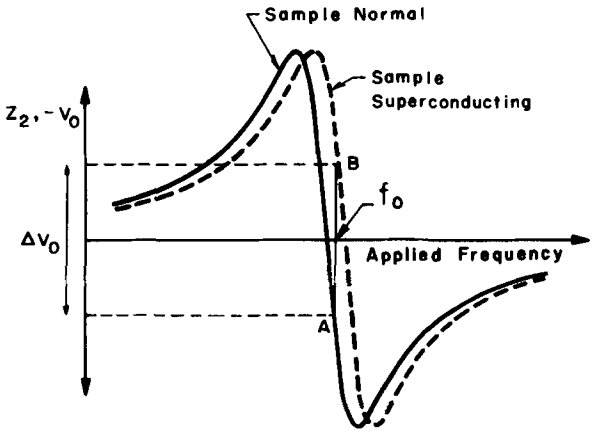

FIG. 1. The frequency dependence (schematic) of the imaginary part of the tuned-circuit impedance Z_2 and the output voltage V_0 as a function of the applied frequency, for the sample in the superconducting and normal states. In operation, the circuit is biased at a fixed frequency f_0 near resonance. The output voltage change when the sample goes from the superconducting state (point B) to the normal state (point A), as shown by ΔV_0.

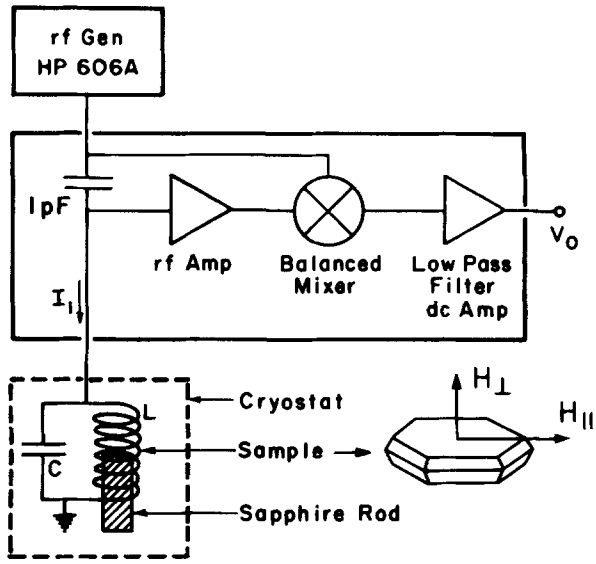

FIG. 2. Block diagram of the detection circuit. A single-crystal sample is also shown (schematically), and the orientations of the dc magnetic field perpendicular ($\perp$) or parallel ($||$) to the plane of the thin platelet sample are indicated. The ac magnetic field is always perpendicular to the sample face.

A typical measured slope of the output curve is $\Delta V_0/\Delta f_r = -30$ mV/kHz, for a Q of 32 and $f_r = 2.8$ MHz. The output noise level, as displayed on the x–y recorder, is approximately 0.1 mV peak-to-peak. (This is equivalent to a frequency shift of 3 Hz.) The noise of our system is due to the input noise of the rf amplifier, which is $\sim 3\ \text{nV/(Hz)}^{1/2}$, close to the state of the art for an input impedance of 30 kΩ. Improved sensitivity $\Delta V_0/\Delta f_r$ may be obtained by using a larger rf current amplitude $|I_1|$ (and, hence, a larger ac magnetic field), or larger Q values. With much larger values of $|I_1|$ or Q, a rf generator of greater stability would be required in order to achieve the better resolution theoretically available.

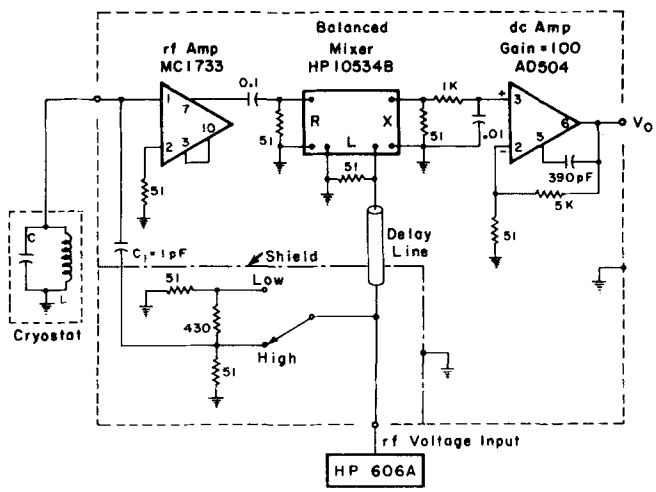

FIG. 3. Detailed schematic of the frequency-shift detection electronics. The two amplifiers are powered by a modular ± 6-V power supply (power supply and connections are not shown). The high-low switch allows the rf current supplied to the LC circuit to be reduced by a factor of 10. All results quoted in this paper are for this switch set in the high position. All the components within the larger dashed box are mounted on a single circuit board in a small aluminum box. Resistances are in ohms and capacitances in μF, unless otherwise noted.

A much larger value of resonant-circuit Q can be obtained with a superconducting coil ($Q \sim 1000$), instead of the copper coil we have used. However, superconducting coils (wound with Nb–Ti wire) were found to be unacceptable even for zero-field measurements because of a large temperature-dependent background signal, apparently due to the temperature dependence of the penetration depth of the superconducting wire. Operation of superconducting coils in large dc fields would clearly be even more problematic.

III. EXPERIMENTAL DETAILS

The apparatus consists of two major components: a dipstick variable-temperature cryostat and the room-temperature electronic detection circuitry. The room-temperature circuitry was described in block diagram form in the previous section; we now discuss circuit details, as shown in Fig. 3. The radio-frequency current souce is a stable rf voltage generator, Hewlett–Packard Model 606A, ($V_g = 0.4$ Vrms)[12a] in series with a 1-pF silvered mica capacitor. The rf voltage across the LC circuit is amplified with a Motorola MC1733 IC video amplifier with a gain $\simeq 30$. A Hewlett–Packard Model 10534B balanced mixer is used. To compensate for extra phase shifts due to the rf amplifier, a 1.7-m section of RG-174/U coaxial cable is used as a time-delay line between the generator and the L port. The rf components present at the output of the mixer are removed with a simple RC low-pass filter having a cut-off frequency of 16 kHz. The dc signal remaining is amplified by an Analog Devices 504M low-noise operational amplifier configured for a gain of 100. The two IC amplifiers are powered by a single $\pm$ 6-V modular power supply. With the exception of this power supply and the HP 606A generator, the entire room-temperature detection circuit is mounted inside a small aluminum box, on a copper-clad printed circuit board which serves as a ground plane. The electronic circuitry has a frequency range of about 50 kHz to 10 MHz. The high-frequency limit is set by the rf amplifier, and the low-frequency limit is set by the balanced mixer.

A schematic diagram of the low-temperature end of the dipstick cryostat probe is shown in Fig. 4. The basic structure is a copper variable-temperature bar located inside a vacuum can. The copper vacuum can is attached with low-melting-point solder, Cerrolow 136 (melting point 136 °F),[13] and can easily be removed. The copper variable-temperature bar is cylindrical, and contains a resistance heater (a 1-kΩ metal-film resistor), a calibrated germanium resistance thermometer,[14] and a capacitance thermometer[15,16] for use in high-magnetic fields. The heater and thermometers are not shown in Fig. 4. A removable copper sample-rod mounting block attaches to the bottom of the variable-temperature bar. The samples are mounted by gluing them onto the end of a cylindrical single-crystal sapphire rod[17] (1.3 mm in diameter or smaller) using rubber cement ("Grippit"), which has been diluted with hexane to a proper consistency. The sample rods are held into holes in the mounting block using 0–80 screws with thermal grease[18] to ensure good thermal contact. Typically, two samples (in two separate coils, each with its own capacitor) are measured during each cooldown.

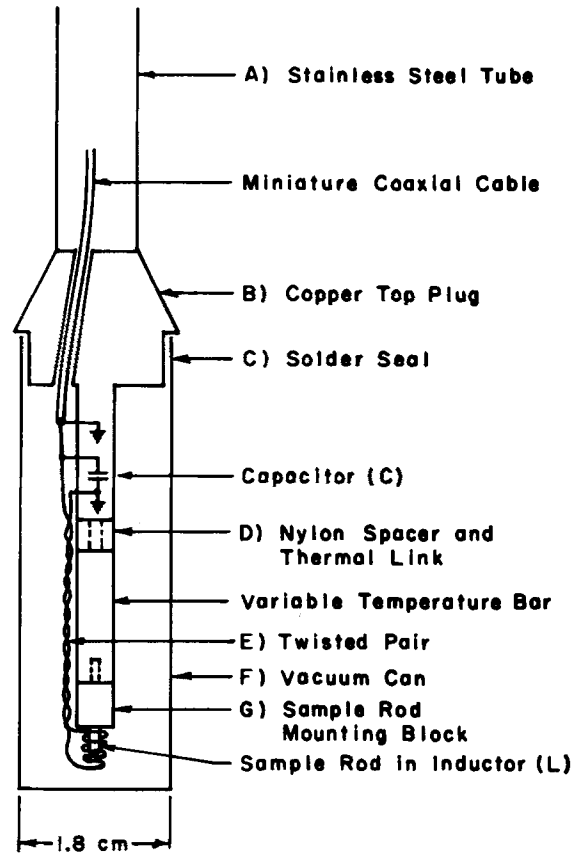

FIG. 4. Schematic diagram of the bottom of the dipstick cryostat (not to scale). (A) Thin-wall, stainless-steel tube. (B) Copper-top plug. This contains several holes for the wires and miniature coaxial cables. (C) Cerrolow 136 solder joint. (D) Thermal link between the copper-top plug and the variable-temperature bar. (E) Twisted pair of No. 34 copper wires connecting L and C. These wires are heat sunk (not shown) by wrapping them around both the variable-temperature bar and the top plug and holding them in place with G. E. 7031 varnish. (F) Copper vacuum can. (G) Removable copper sample-rod mounting block. The heater and thermometers are not shown. Only one sample rod, coil, capacitor, etc. are shown, although the cryostat actually contains two sets.

The variable-temperature section is connected to the copper-top plug by a 4–40 brass screw passing through a 0.5-cm-long nylon spacer. The brass screw acts as a structural member and also as a weak thermal link to the bath temperature. A number of small copper wires, mostly 80 μm in diameter, pass from the top plug to the variable-temperature bar. These wires are wrapped and heat sunk on both sides of the nylon spacer using General Electric 7031 varnish. It is the thermal conductance of the brass screw and the copper wires which sets the practical upper limit of the cryostat's useful temperature range. For the wires and brass screw used, a heater power of 8 mW is required to reach a temperature of 7 K with the bath at 4.2 K, while 150 mW is required to reach 20 K.

The inductor slips over the end of the sapphire rod to enclose the sample at its center. Thus, the ac field is always oriented perpendicular to the face of the sample. The capacitor is mounted on the top plug to keep it at as constant a temperature as possible, since the capacitance value is slightly temperature dependent. The tuned circuit is electrically grounded at this point by soldering one side of the capacitor to the top plug. This also provides an effective method of heat sinking the capacitor.

The requirements on the capacitor to be used in the LC circuit are that it must have a high Q and a large self-resonant frequency, yet be small enough to fit in the vacuum can. A small temperature coefficient of capacitance (at liquid He temperatures) is also highly desirable. For this last requirement, silvered-mica capacitors would be ideal, as they have essentially a zero-temperature coefficient. However, ceramic capacitors manufactured by American Technical Ceramics[19] have been used because their much smaller size allows larger values of capacitance (1 to 5 nF) to be used. The inductors typically have inductances between 0.5 and 1 μH and are usually wound from 80-μm-diam copper wire (two layers of 10 turns each). The inductor must be small enough to ensure a reasonable filling factor, yet have enough inductance to achieve a reasonable Q.

Resonant frequencies between 2 and 4 MHz are obtained, and Q values are typically about 30. For the various coils used, the calculated rf magnetic field is between 0.01 and 0.1 G.[20] This small ac field magnitude is dictated by our samples, where the transitions can be depressed by much larger ac fields.

The capacitor and inductor have a Q of approximately 60 (at 4.2 K) when connected directly together. The resistance of the twisted pair of 160-μm-diam copper wires which connects L and C in the apparatus lowers the Q to approximately 45. Losses in the coaxial cable from the low-temperature end of the cryostat to the top of the cryostat, and from that point to the electronics cause a further reduction of Q to a value of approximately 30. A miniature coaxial cable[21] is used in the cryostat to satisfy space requirements and to minimize the heat leak to the helium bath. Low-capacitance coaxial cable (type RG-62/U) is used to connect the cryostat to the room-temperature electronics to minimize additional degradation of the circuit Q.

The room-temperature end of the dipstick contains two hermetic 10-pin electrical feedthroughs, a thermocouple pressure gauge, an overpressure release valve, and a pump line through which gas can be added to or pumped from the cryostat. For surveying the transition temperatures of a large number of samples, the cryostat can be placed directly in a wide-mouth liquid-helium storage Dewar (for $T_c > 4.2$ K). If the cryostat is lowered slowly, liquid-helium consumption can be below 1 liter per cool down.

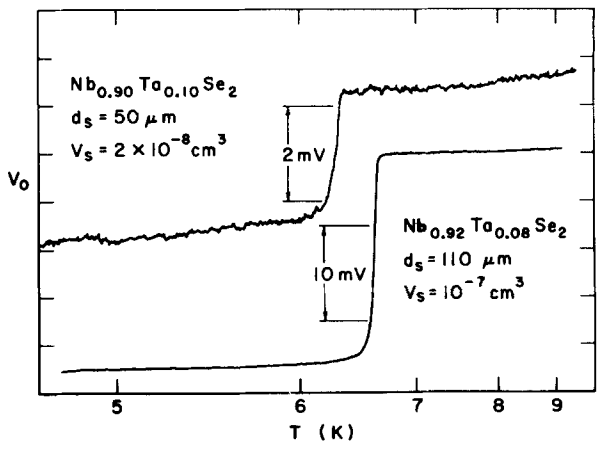

FIG. 5. The zero-field transitions, V_0 as a function of temperature, for two samples, a 50-μm-diam hexagonal crystal of $Nb_{0.90}Ta_{0.10}Se_2$ and a 110-μm-diam hexagonal crystal of $Nb_{0.92}Ta_{0.08}Se_2$. Both samples have the shape of a thin hexagonal platelet, as shown schematically in Fig. 2, and are approximately 10 μm thick.

In order that the shape of the transition be accurately recorded, it is necessary to operate near the resonant frequency where the transfer curve shown in Fig. 1 is linear. This requirement can be met by operating sufficiently near to f_r that the output voltage never exceeds 1/2 of the peak value. It is also important that losses in the sample have a negligible influence on the Q of the circuit, otherwise the measured transition curve will be distorted. For larger samples, losses in the sample can influence Q, and the change in V_0 can be so large that it moves completely off the linear portion of the transfer curve. Both of these problems can be solved by adding a shunting resistor across the LC circuit at the room-temperature end of the cryostat. This lowers the Q, and thus increases the frequency range over which V_0 is linear.

IV. SYSTEM PERFORMANCE

As an illustration of the sensitivity of this apparatus, we show in Fig. 5 the zero-field transitions as a function of temperature for two small crystals. The first crystal of $Nb_{0.90}Ta_{0.10}Se_2$ is a thin hexagonal platelet with a diameter of 50 μm and a thickness of about 10 μm (sample volume $V_s = 2\times10^{-8}$ cm^3). As can be seen, the signal-to-noise ratio of $\simeq$20 is sufficient to allow the transition temperature to be determined accurately. Also shown in Fig. 5 is the zero-field transition of a somewhat larger sample, a 110-μm-diam hexagonal crystal of $Nb_{0.92}Ta_{0.08}Se_2$. For a sample of this size, the noise is barely perceptible.

The slope of the trace above and below the transition for the smaller sample in Fig. 5 is due to a small instrumental background signal. The slope of this background signal increases considerably above about 8.5 K. This background signal is caused primarily by the temperature dependence of the capacitance. Even though the capacitor is nominally at a fixed temperature, its temperature does change slightly as the temperature of the variable-temperature bar is varied. The background signal seen in Fig. 5 could be reduced by better thermal isolation of the capacitor or by the use of a silvered-mica capacitor. The instrumental background signal can also be significantly reduced by the presence of a small pressure (10–20 mTorr) of helium exchange gas in the vacuum can.

Sensitive operation of the apparatus in large magnetic fields is also possible. Figure 6 shows transition curves for two samples with the magnetic field oriented perpendicular ($\perp$) or parallel ($\parallel$) to the plane of the thin hexagonal-platelet samples. The arrows in Fig. 6 show the direction of the temperature sweep. The hysteresis seen in the mixed region below the main transition is an intrinsic effect; its origin is discussed below. (The hysteresis is not shown in Fig. 6 for the $H_\parallel$ transition.) No hysteresis is seen in zero-field transition curves. We find that the main transition of each of these curves occurs at the temperature corresponding to the upper critical field boundary. We thus identify the midpoint of this main transition as $T_{c2}(H)$. The evidence in favor of this identification is the agreement of our ac susceptibility transitions

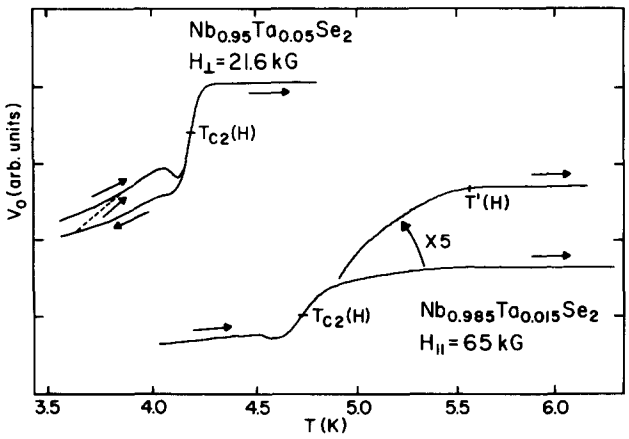

FIG. 6. The transitions of two samples in dc fields; a crystal of $Nb_{0.95}Ta_{0.05}Se_2$ in a 21.6-kG field oriented perpendicular to the face of the sample, and a crystal of $Nb_{0.985}Ta_{0.015}Se_2$ in a parallel field of 65 kG. The arrows along the curves indicate the direction of the temperature sweep. For the parallel field orientation, V_0 is also shown on a five-times-expanded vertical scale above the main transition. The high-temperature tail is a surface superconductivity effect. [The temperature $T'(H)$ defines a field $H(T')$ which scales as expected from the theory of surface superconductivity; $H_{c3}(T) = 1.7H_{c2}(T)$.]

for the *pure* compound $NbSe_2$ with H_{c2} data obtained previously with the specific-heat technique[8] on larger crystals of $NbSe_2$. The substitutional alloy crystals $Nb_{1-x}Ta_xSe_2$ display susceptibility transition shapes very much like those of $NbSe_2$. Values of $H_{c2}(T)$ for the alloy crystals are close to those of pure $NbSe_2$, with small, systematic changes as a function of alloy composition x.

The hysteretic behavior seen in Fig. 6 is probably caused by an intrinsic barrier to flux entry into a type-II superconductor in the mixed state. The surface barrier to flux exit can be smaller in magnitude.[6] An asymmetric barrier could affect the dc field distribution near the surface in such a way as to cause the hysteresis seen in Fig. 6, assuming that the very small ac field probes predominantly the surface of the sample.[7]

As seen in Fig. 6, when the dc field is oriented parallel to the face of the sample, V_0 continues to increase somewhat over a finite temperature interval above the main transition. The field dependence of the high-temperature end of the tail [denoted as $T'(H)$], indicates that this small effect is due to surface superconductivity, as $T'(H)$ is close to $T_{c3}(H_{||})$. [We recall that $H_{c3}(T) = 1.7H_{c2}(T)$.] This finding provides additional evidence that the main transition corresponds to $H_{c2}(T)$.

For operation in a large dc field there is a background signal (at a fixed temperature) which changes with the dc field. Changes in this background signal during a field sweep are much larger than the temperature-dependent background signal measured in a fixed dc field. Thus, temperature sweeps in a fixed field are employed for all our measurements. Other than the field-dependent background signal, the major way in which operation of the detection circuit is affected by the dc field is that the Q, and thus the sensitivity, of the resonant circuit is decreased, because of the magnetoresistance of the copper wire in the coil. The Q decreases roughly linearly as the field increases, typically being reduced to 75% of the zero-field value at 70 kG.

In large fields, the dc noise level is not increased, provided that the cryostat is held rigidly in the center of the solenoid. This is accomplished with a ring of beryllium–copper "fingers" mounted on the top of the magnet. Operation at fields to 150 kG was carried out at the National Magnet Laboratory using a Bitter solenoid. It was found necessary to use a field stabilizer with this Bitter solenoid, thereby reducing field fluctuations to a fractional value $< 10^{-5}$. Without this stabilizer, random field fluctuations produced eddy current heating of the variable-temperature bar, precluding a slow and uniform sweep of the temperature.

ACKNOWLEDGMENTS

We would like to thank B. Hanson for assistance in building the room-temperature electronics, and L. G. Rubin for helpful comments on this manuscript. Studies above 80 kG were performed while the authors were guest scientists at the Francis Bitter National Magnet Laboratory, which is supported at the Massachusetts Institute of Technology by the National Science Foundation. This research was supported by NSF grants DMR-7609591, DMR-7817957, and DMR-8207443.

[1] R. Bachmann, F. J. Disalvo, Jr., T. H. Geballe, R. L. Green, R. E. Howard, C. N. King, H. C. Kirsch, K. N. Lee, R. E. Schwall, H. U. Thomas, and R. B. Zubeck, Rev. Sci. Instrum. **43**, 205 (1972); R. E. Schwall, R. E. Howard, and G. R. Stewart, *ibid.* **46**, 1054 (1975).
[2] G. D. Zally and J. M. Mochel, Phys. Rev. B **6**, 4142 (1972); N. A. H. K. Rao, E. D. Dahlberg, A. M. Goldman, L. E. Toth, and C. Umbach, Phys. Rev. Lett. **44**, 98 (1980).
[3] G. R. Stewart, Rev. Sci. Instrum. **54**, 1 (1983).
[4] See, for instance, M. Tinkham, *Introduction to Superconductivity* (McGraw-Hill, New York, 1975).
[5] M. Strongin, D. G. Schweitzer, A. Paskin, and P. P. Craig, Phys. Rev. **136**, A926 (1964).
[6] J. F. Bussiere, Phys. Lett. A **58**, 343 (1976); C. P. Bean and J. D. Livingston, Phys. Rev. Lett. **12**, 14 (1964); J. R. Clem, in *Low Temperature Physics (LT-13)*, edited by K. D. Timmerhaus, W. T. O'Sullivan, and E. F. Hammel (Plenum, New York, 1974), Vol. 3, p. 102; R. W. DeBois and W. DeSorbo, Phys. Rev. Lett. **12**, 499 (1964); H. A. Ullmaier and W. F. Gauster, J. Appl. Phys. **37**, 4519 (1966).
[7] B. J. Dalrymple and D. E. Prober, J. Low Temp. Phys. (submitted); Bull. Am. Phys. Soc. **27**, 157 (1982); B. J. Dalrymple, Ph. D. thesis, Yale University, 1983. (Available from University Microfilms, Ann Arbor, MI 48106.)
[8] R. E. Schwall, G. R. Stewart, and T. H. Geballe, J. Low Temp. Phys. **22**, 557 (1976).
[9] (a) D. S. McLachlan and J. Feder, Rev. Sci. Instrum. **39**, 1340 (1968); (b) R. F. R. Pereira, E. Meyer, and M. F. da Silveira, *ibid.* **54**, 899 (1983).
[10] A. L. Schawlow and G. E. Devlin, Phys. Rev. **113**, 120 (1959); D. M. Gualtieri, Rev. Sci. Instrum. **49**, 1716 (1978).
[11] A. T. Skjeltorp and W. P. Wolf, Phys. Rev. B **8**, 215 (1973); F. Rothwarf, D. Ford, and L. W. Dubeck, Rev. Sci. Instrum. **43**, 317 (1972).
[12] C. T. Van Degrift, Rev. Sci. Instrum. **46**, 599 (1975). If the HP 606a generator is not available, other generators, such as rf synthesizers, would have adequate frequency and amplitude stability for this application.
[13] Cerro Copper and Brass Co., Bellefonte, PA 16823.
[14] Model CR-1000, Cryocal Inc., Minneapolis, MN 55435.
[15] Model CS-400 GR, Lake Shore Cryotronics, Inc., Columbus, OH 43229.
[16] L. G. Rubin and W. N. Lawless, Rev. Sci. Instrum. **42**, 571 (1971); D. E. Prober, *ibid.* **50**, 387 (1979).
[17] Tyco Saphikon Division, Milford, NH 03055.
[18] Dow Corning Silicone High Vacuum Grease, Dow Corning Corp. Midland, MI 48640.
[19] American Technical Ceramics, Huntington Station, NY 11746.
[20] These ac fields, and all the results quoted in this paper, are for the switch in Fig. 3 set in the "high"position.
[21] Type-M ultraminiature coaxial cable, Lake Shore Cryotronics, Columbus, OH 43229.